Intergranular diffusion rates from the analysis of garnet surfaces: implications for metamorphic equilibration

Tim J. Dempster, Shona Symon[1] & Peter Chung

School of Geographical and Earth Sciences, University of Glasgow, Glasgow G12 8QQ, UK.

[1.] Present address: Department of Civil and Environmental Engineering, University of Strathclyde, Glasgow G1 1XJ, UK.

ABSTRACT

Novel approaches to garnet analysis have been used to assess rates of intergranular diffusion between different matrix phases and garnet porphyroblasts in a regionally metamorphosed staurolite-mica-schist from the Barrovian-type area in Scotland. X-ray maps and chemical traverses of planar porphyroblast surfaces reveal chemical heterogeneity of the garnet grain boundary linked to the nature of the adjacent matrix phase. The garnet preserves evidence of low temperature retrograde exchange with matrix minerals and diffusion profiles documenting cation movement along the garnet boundaries. Garnet-quartz and garnet-plagioclase boundaries preserve evidence of sluggish Mg, Mn and Fe diffusion at comparable rates to volume diffusion in garnet, whereas diffusion along garnet-biotite interfaces is much more effective. Evidence of particularly slow Al transport, probably coupled to Fe^{3+} exchange, is locally preserved on garnet surfaces adjacent to Fe-oxide phases. Ca distribution on the garnet surface shows the most complex behaviour, with long wavelength

heterogeneities apparently unrelated to the matrix grain boundaries. This implies that the Ca content of garnet is controlled by local availability and is thought likely to reflect disequilibrium established during garnet growth. Geochemical anomalies on the garnet surfaces are also linked to the location of triple junctions between the porphyroblasts and the matrix phases, and imply enhanced transport along these channels. The slow rates of intergranular diffusion and the characteristics of different boundary types may explain many features associated with the prograde growth of garnet porphyroblasts. Thus minerals such as quartz, Fe-oxides and plagioclase whose boundaries with garnet are characterized by slow intergranular diffusion rates appear to be preferentially trapped as inclusions within porphyroblasts. As such grain boundary diffusion rates may be a significant kinetic impediment to metamorphic equilibrium and garnet may struggle to maintain chemical and textural equilibrium during growth in pelites.

Keywords: garnet, intergranular diffusion; porphyroblast surfaces; retrograde equilibration; grain boundaries.

INTRODUCTION

The transport of chemical components within rocks is recognized as a rate limiting process during metamorphism that facilitates the growth and dissolution of minerals and allows equilibrium to be established between phases (Mueller *et al*., 2010; Carlson *et al*., 2015a). Volume diffusion within minerals is known to be relatively slow in metamorphic conditions as demonstrated by the preservation of growth zoning of cations in many metamorphic porphyroblasts (e.g. Kohn, 2003). However there is often a general assumption that the rates of

intergranular diffusion are relatively fast (Joesten, 1991; Dohmen & Milke, 2010). In part this contributes to the belief that thermodynamic equilibrium between minerals is readily attained during prograde metamorphism. Despite this assumption, evidence for disequilibrium in metamorphic rocks suggests that kinetic factors, such as transport along grain boundaries, may be important rate-controlling steps in attainment of metamorphic equilibrium and porphyroblast growth (Carlson, 1989; Carlson, 2002; Pattison & Tinkham, 2009; Mueller *et al*., 2010; Pattison *et al*., 2011; Carlson *et al*., 2015b). The uncertainty associated with rates of intergranular transport is compounded by the relative paucity of estimates for grain boundary diffusion rates in either natural samples or from diffusion experiments relevant to common rock types and geochemical species (Brady, 1983; Florence & Spear, 1995; Dohmen & Milke, 2010; Marquardt *et al*., 2011; Okudaira *et al*., 2013; Bromiley & Hiscock, 2016). Other characteristics of grain boundary interfaces, such as permeability and effective solubility of components in the intergranular medium are recognized as important controls on reaction mechanisms (Dohmen & Chakraborty, 2003), but some of these are also rather poorly constrained.

Garnet is the most commonly studied metamorphic phase, in part because of it has relatively sluggish volume diffusion rates for divalent cations (Chakraborty & Ganguly, 1992; Carlson, 2006; Vielzeuf *et al*., 2007; Ganguly, 2010). Hence garnet has an ability to preserve changing chemistry during growth and potentially to record the evolution of pressure and temperature during metamorphic events. However many studies have demonstrated evidence of volume diffusion in garnet at elevated temperatures (Woodsworth, 1977; Yardley, 1977) and associated exchange during retrograde cooling (Tracy, 1982; Dempster, 1985;

Ehlers *et al*., 1994; Florence & Spear, 1995). Recognition of such diffusive re-equilibration is important for the assessment of peak metamorphic P-T conditions (Spear, 1991; Florence & Spear, 1991; Kohn & Spear, 2000; Caddick *et al*., 2010); metasomatic changes within the effective whole rock composition (Spear, 1988; Florence & Spear, 1993); and, geospeedometry and the determination of the duration of metamorphic events (Lasaga, 1983; Ague & Baxter, 2007; Caddick *et al*., 2010; Müller *et al*., 2015).

The study and identification of minerals using thin sections (Sorby, 1851) has become an essential and integral part of geoscience (Vernon, 2004) and the technique is at the heart of many, perhaps most, petrological advances. However the dominance of this approach has created an ingrained and inevitable emphasis on the study of the interiors of the minerals. Arguably this has occurred at the expense of understanding grain boundary processes.

Using a new approach to mineral analysis, this study attempts to assess the rates of intergranular diffusion along garnet grain boundaries. We use traditional techniques to analyze garnet composition in 1D profiles perpendicular to the grain boundaries in combination with 2D X-ray mapping of sections through the central parts of the porphyroblasts to monitor volume diffusion. In a novel approach we also map compositional gradients in one and two dimensions on the exposed surfaces of porphyroblasts to constrain rates of chemical transport along garnet-matrix grain boundaries.

GEOLOGICAL SETTING AND PETROGRAPHY

The Late Proterozoic Dalradian schists in the Scottish Highlands experienced peak regional metamorphic conditions during the Ordovician (Oliver *et al*., 2000;

Dempster *et al*., 2002), although parts of the succession have also experienced earlier Precambrian deformation and metamorphism (Dempster & Jess, 2015). Sample GL774 is of a staurolite garnet mica schist from the kyanite zone in the Barrovian type area (Barrow, 1893) in Glen Effock at the north end of Glen Esk, eastern Scotland (UK grid ref NO 4238377169). The schist contains some <1 cm thick quartz-rich layers but generally is biotite- and muscovite-rich with large (up to 3 mm diameter) garnet porphyroblasts (Fig. 1) and smaller 1 mm long staurolite concentrated within the thicker micaceous layers. In thin section view, garnet porphyroblasts are typically equant with planar gently curving grain boundaries (Fig. 1). Some have locally irregular margins characterized by embayments (up to 1 mm wide) filled with aggregates of granoblastic plagioclase and quartz, with minor muscovite and staurolite. Micas are strongly aligned and typically partially wrap around the garnet porphyroblasts, which contain abundant small inclusions, mostly of quartz and Fe-oxides that define a weak alignment at a high angle to the external fabric elements (Fig. 1). The outer ~100 μm edge of the garnet porphyroblasts is typically inclusion free (Fig. 1). The sample lacks major retrograde alteration although Fe-staining is present on some grain boundaries and small clusters of unaligned retrograde chlorite after biotite are locally present. The schist contains 27% quartz, 26% biotite, 15% muscovite, 13% garnet, 11% plagioclase, 3% staurolite and 3% chlorite and minor Fe-oxides with accessory apatite, zircon and tourmaline.

Conditions of peak regional metamorphism are estimated as ~600 ^{o}C and 0.6 GPa (Harte & Hudson, 1979; Vorhies & Ague, 2011) and evidence from garnet zoning profiles and X-ray maps suggests that re-equilibration of garnet zoning profiles via volume diffusion has occurred in the rocks (Dempster, 1985; Vorhies

126 & Ague, 2011; Viete *et al*., 2011). Garnet zoning profiles are progressively
127 smoothed during metamorphism and in this area, localized low Mg/Fe garnet
128 rim compositions are associated with exchange occurring at low temperature
129 with adjacent biotite (Dempster, 1985). Estimated biotite and garnet exchange
130 reaction geothermometry based on "rim-rim" compositions suggests that
131 equilibration may continue from peak temperature conditions to temperatures
132 of less than 500 ^{o}C (Dempster, 1985). Some studies have suggested that the
133 rocks in this area experienced very short times close to maximum temperatures
134 (Oliver *et al*., 2000; Ague & Baxter, 2007). However the lack of well-constrained
135 ages of deposition or information on the nature of original compositional zoning
136 in garnet and apatite mean that well-constrained prograde thermal histories for
137 these rocks are not available.
138
139 **METHODS**
140 A combination of conventional polished thin section analysis and the analysis of
141 flat crystal surfaces and associated matrix surfaces was used to characterize the
142 sample. The mineral surfaces were produced by snapping of thin 4mm rock
143 slices (cf. Lawther & Dempster, 2009). This thickness proved to be optimum for
144 creating a clean snap perpendicular to the rock cleavage, thus exposing
145 porphyroblasts surfaces and intact adjacent matrix. Typically slices were cut
146 perpendicular to the rock cleavage and then snapped, also perpendicular to the
147 cleavage. Initial inspection of the snapped surfaces was done using a binocular
148 microscope and apparently suitable surfaces of porphyroblast and intact
149 adjacent matrix were selected. Pairs of slices were then stuck together with resin
150 with the porphyroblast and matrix "hole" in close proximity. Rock surfaces were

coated with relatively thick carbon layers (ca. 60 nm) to ensure electron conductivity across the irregular surfaces. Samples were initially characterized using a FEI Quanta 200F field emission environmental scanning electron microscope operated at 20 kV to allow further selection of the most appropriate porphyroblast surfaces. These were then analysed using a Carl Zeiss Sigma VP electron microscope at 20 kV with Oxford instruments X-Max 80 energy dispersive spectrometry with overnight, typically 15 hour, analysis to acquire X-ray maps and traverses with minimized errors. Analyses of mineral surfaces are done using energy dispersive spectrometry because the geometry of the analytical system is less sensitive to surface irregularity and orientation variations.

Porphyroblasts that form positive relief areas and the adjoining matrix "hole" were both characterized using secondary and backscattered electron images. The topographic surfaces of porphyroblasts and matrix were examined to ensure that the snap occurred without any significant loss of intervening material. As such most of the exposed garnet surfaces, and all of those analyzed, represent grain boundaries between porphyroblasts and the adjacent matrix. Digital elevation models were produced using Alicona Mex 3D software from stereo-pairs of secondary electron images of the garnet porphyroblasts. This allowed flat garnet surfaces with minimum relief to be selected for analysis. This also enabled the garnet surface to be leveled at the analytical working distance and oriented to avoid shielding by adjacent matrix minerals on the irregular surface to ensure clear line of sight to the X-ray detector and hence optimizing the X-ray yield. Surface profiles were obtained from the digital elevation models for some surfaces so that topographic artifacts of the geochemical traverses could be

identified. Several surfaces were also analyzed in a variety of orientations to ensure that none of the compositional variations are artifacts of the geometry of surface. Backscattered electron images of the matrix surface adjacent to the exposed garnet surface were superimposed onto the images of the garnet surface so that chemical maps and compositional traverses across the garnet surfaces could be directly linked to the locations of adjoining matrix phases and the position of their grain boundaries. Grain boundaries between different minerals were easy to identify using backscattered electron images and some of those between minerals of the same type could be identified when an internal structure such as cleavage could be used to identify individual grains. Those between minerals lacking a prominent internal structure, such as quartz, are more difficult to identify using the imaging techniques employed in this study. Compositions of the garnet surfaces were assessed in traverses perpendicular to the orientation of adjacent grain boundaries in the matrix to characterize a range of different grain boundary types. Typically surfaces selected to avoid topographic steps and surface blemishes yielded the chemical profiles that are thought to represent the composition of the garnet surface most reliably.

RESULTS

Internal zoning of garnet

Geochemical analysis of polished thin sections of the interior of garnet porphyroblasts reveal them to be zoned with smooth chemical variations from core to rim (Fig. 2). They are characterized by relatively high Mn content cores (Fig. 2b), with progressively increasing Mg/Fe from core towards the rim with local decrease in Mg/Fe immediately adjacent to the rim in the outer $\sim$50 μm.

Cores of the porphyroblasts are also relatively Ca-rich (Fig. 2c), although zoning patterns for Ca are less obviously concentric than the other major divalent cations. The edge of the garnet porphyroblasts is characterized by a low Mg content in the outer 10-20 μm adjacent to biotite (Fig. 2d), but rim compositions are variable and correlated with adjacent mineral type. Generally garnet adjacent to quartz lacks well-developed edge-related zoning. Mn- and Ca-contents are typically slightly elevated towards the outer edge of the garnet (Fig. 2a,b). The analysis of the absolute edge of the porphyroblast is limited by the interaction volume of the electron beam and proximity to grain boundary. Hence analyses within 2 μm of the grain boundary are in part artifacts of the boundary.

Surface morphology of garnet

Secondary electron images of snapped rock samples show that garnet surfaces preserve a combination of extensive flat surfaces, and slightly more irregular surfaces containing a variety of small steps and growth facets (Fig. 3a,b). There is no evidence from the surface morphology of the porphyroblasts that they might represent multiple crystals (cf. Whitney *et al*., 2008). The growth steps often mirror the topography of the matrix on the opposite surface (Fig. 3d). Although plagioclase grain boundaries often show porous surfaces characterized by ~5 μm pores (cf. Lawther & Dempster, 2009), most other matrix phases have smooth planer boundaries. Growth steps and facets on garnet surfaces (Fig. 3b) may coincide with matrix grain boundaries but more frequently the topography of the porphyroblast surface is independent of the geometry of the grain boundary network in the adjacent matrix (Fig. 3d). As such grain boundaries between minerals on the matrix surface frequently coincide with perfectly planar parts of the garnet surface (Fig. 3b,c). Some growth steps create small

ridges and have an influence on the chemistry of the garnet recorded across that step, however wherever possible traverses were selected in an attempt to avoid significant topographic irregularity. The effect of slight variations in the topography of the surface on the garnet chemistry depends in part on the orientation of the traverse relative to the spectrometer but is typically most marked for the lower atomic number elements and is interpreted to reflect preferential X-ray absorption (Reed, 2005). The detailed small-scale topographic features of these surfaces (Figs. 3b & 4) are hidden in conventional thin section petrography and disguised by an apparently gently curving geometry displayed by the porphyroblasts shapes (Fig. 1). These garnet and matrix surfaces are often very clean in secondary electron images. However, locally either surface may show bright BSE image deposits of Fe-oxides (Fig. 4), which may occur in small isolated spots or as more continuous thin films, other surfaces may have small clusters of S-rich deposits. Wherever possible the traverses were sited to avoid these surface deposits. The Fe-rich grain boundary deposits appear as thin discontinuous brown-orange streaks on some grain boundaries within thin sections. The thin films of Fe-oxide coating garnet surfaces appear to have little effect on the garnet compositions analysed other than when coarser grained aggregates of oxides are present (e.g. Fig. 6b). In such instances analysed compositions show more variability, especially in the low atomic number elements. The mineral volume activated under the electron beam is largely just below the surface (Reed, 2005) and the influence of the coarser deposits may be more of a topographic effect on X-ray absorption.

General chemical characteristics of the garnet surfaces

The X-ray maps of garnet surfaces show a patchy distribution of divalent cations, especially those of Mg and Mn, that is typically spatially linked to the nature of the adjacent matrix minerals. The variation in the garnet composition, expressed as end member components, of the porphyroblast surface is approximately ±6% X_{prp}; ±2% X_{sps}; ±6% X_{alm}; ±2% X_{grs}. Some compositional "boundaries" on the garnet surface are sharp with locations closely matching the positions of phase boundaries in the adjacent matrix (Fig. 5). Garnet surfaces adjacent to Fe-oxide in the matrix shows some of the sharpest compositional "boundaries" with low Al content only matched by high Fe in the garnet. The maps of chemical variation on the garnet surface closely mirror the grain boundaries of the adjacent Fe-oxide (Fig. 5). As such there is no evidence to suggest that significant recrystallization of the matrix phases has occurred after the chemistry of the garnet surface was established. Other garnet surfaces show more gradual compositional changes perpendicular to the orientation of the mineral boundaries in the matrix.

Overall the X-ray maps of Mg show the most pronounced variations on the garnet surfaces that can be systematically linked to the location of matrix grain boundaries (Fig. 6). Typically high Mg contents of garnet are matched by low Mn and Fe contents. High Ca contents may be associated with elevated Mg contents but such patterns are less consistent. Although typically the changes in surface composition of garnet are very closely matched to the positions of grain boundaries in the adjacent matrix some are apparently slightly offset by a few microns. In part this may reflect the 3-D sub-surface geometry of the grain boundary within the analytical volume and in part it is caused by distortion of

the electron images due to the different geometry of the porphyroblast surface and the matrix surface relative to the electron beam.

Geochemical characteristics of specific grain boundaries

Garnet-biotite-quartz (Mg-Mn-Fe variation)

Garnet adjacent to biotite has a consistently low Mg and high Mn and Fe contents relative to that adjacent to quartz or plagioclase (Fig. 7). Line scans of the Mg content of the garnet surface across the position of biotite-quartz grain boundaries within the adjacent matrix reveal that the garnet composition gradually changes in a smooth exponential profile marked by a increase in Mg/Fe along the garnet-quartz boundary away from the biotite and a decrease in Mg/Fe along the garnet-biotite boundary away from the quartz (Fig. 6). The compositional changes are typically more gradual within the garnet adjacent to biotite occurring over a distance of ~ 50 μm and show a sharper transition in Mg content over a distance of ~ 20 μm away from the quartz-biotite junction along the garnet-quartz boundary (Fig. 6b,c). Traverses of the garnet surface across quartz-biotite boundaries parallel to and perpendicular to the trace of the [001] cleavage in biotite show similar changes in garnet chemistry, although compositional changes appear to be spread over a longer distance in traverses parallel to biotite cleavage (Fig. 6c). Mn and Fe contents of garnet also show significant variation, mirroring the variation in Mg contents, linked to the adjacent matrix phase with elevated Mn next to biotite and profiles typically showing a smooth decrease in concentration along boundaries away from the biotite (Fig. 6). Although most of the analysed profiles show similar geochemical trends some differences are present. Some compositional traverses along quartz-garnet boundaries away from biotite appear to plateau at lower concentrations

of Mg (Fig. 6c). In other traverses Mn contents may show rather limited variation and the changes in Mg content of the garnet surface are dominantly matched by variation in the Fe content (Fig. 6b).

Garnet-biotite-plagioclase (Mg-Mn-Fe variation)

Garnet surfaces adjacent to biotite-plagioclase grain boundaries display similar characteristics to those adjacent to biotite-quartz boundaries with sharp exponential Mg-compositional gradients mirrored by more gradual Mn- and Fe-compositional profiles (Fig. 7). The Mg variation occurs over a very similar scale (~ 10 μm) along the garnet-plagioclase boundary to the garnet-quartz boundaries.

Garnet-muscovite-quartz (Mg-Mn-Fe variation)

Garnet adjacent to muscovite typically has a composition that is intermediate between that adjacent to quartz and that adjacent to biotite. Quartz-muscovite boundaries typically lack systematic differences in garnet composition between the garnet-muscovite interface and the garnet-quartz interface. However, there are changes in the garnet composition that are directly linked to the position of the muscovite-quartz boundary itself. Locally elevated Mn-contents of the garnet surface are associated with quartz-muscovite-garnet triple junctions (Fig. 8). This geochemical anomaly is matched by lower Mg-contents, and this typically has a less smoothed sharper anomaly. The wavelength of the high Mn-, low Mg-anomaly varies from 20 μm (Fig. 8c) to 5 μm (Fig. 8d) between different grain boundaries and may be linked to the orientation of the boundary or the orientation of the muscovite lattice. These anomalies may display an asymmetry with geochemical variation in profiles along the muscovite-garnet boundary occurring over longer distances in comparison to that along the quartz-garnet

boundary. This is especially the case when the traverse is parallel to the cleavage of the muscovite (Fig. 8c). Apart from the changes in composition linked to the position of the matrix grain boundary itself, the garnet surface along quartz-muscovite interfaces appears to be characterized by smooth longer wavelength geochemical variations (e.g. Mg in Fig. 8d).

Ca variation on the garnet surface

The Ca-contents of the garnet surface show the least systematic variation with evidence of a lack of equilibrium characterized by smooth, long-wavelength, low-amplitude variations in composition (Figs. 6a & 7). These variations occasionally appear related to adjacent grain boundaries with sharp transitions over a distance of ~ 10 μm (Fig. 6a) but in most traverses the Ca minima and maxima that occur on the garnet surface are unrelated to either the position of the grain boundaries in the matrix or the nature of the adjacent phase (Fig. 7). Garnet adjacent to plagioclase shows no obvious influence of exchange of Ca but, as with some other boundary types, gradual variation in the Ca content is preserved in garnet (Fig. 7).

INTERPRETATION

Smooth compositional profiles are retained in the interior of the garnet porphyroblasts and are interpreted as growth zoning with partial modification through volume diffusion (e.g. Kohn, 2003). Low Mg garnet rim compositions record post peak metamorphic exchange with adjacent matrix biotite (e.g. Tracy, 1982; Kohn & Spear, 2000). The presence of smoothly curving compositional profiles is indicative of exchange via volume diffusion rather than fluid-related chemical modification via coupled dissolution-reprecipitation processes. Such

garnet zoning is identical to that reported by Dempster (1985) and Viete *et al*. (2011) from this area and confirms the localized retrograde exchange between garnet and some other matrix phases.

Intergranular diffusion along garnet surfaces

Similarly smooth compositional profiles are recorded by the garnet surfaces, which have partially equilibrated through intergranular diffusion.

Different elements show different diffusion profiles on the garnet grain boundaries; different boundary types show different diffusion profiles; and, the diffusion profiles may be partially dependent on the orientation of the boundary or the phyllosilicate lattice. Some profiles show chemical variation directly linked to the position of the immediately adjacent grain boundary (e.g. Mg and Mn across the quartz-biotite boundaries). Other parts of the garnet surface show chemical variation that is apparently not systematically linked to the immediately adjacent grain boundaries (e.g. some Ca variation). Generally the consistent profiles displayed by the same boundary types argues that diffusive movements are subject to the same controls and hence that the intergranular regions (cf. Brady, 1983) themselves have similar properties irrespective of their orientation or the crystal lattice orientation.

Adjacent to Fe-oxides within the rock, rather than the grain boundary films, the garnet surface is depleted in Fe and enriched in Al (Fig. 5). This may reflect exchange in the trivalent lattice site of garnet. This exchange may be associated with retrograde processes, as the Fe-oxide in this instance has a rather ragged texture characteristic of formation during late alteration. The geochemical boundaries of this modified garnet are exceptionally sharp and this implies low

rates of Al and Fe^{3+} intergranular diffusion (cf. Carmichael, 1969) and sluggish movement relative to rates of Fe^{2+}, Mg, Mn, and Ca grain boundary diffusion. Mg variation on the garnet surface typically records the most complete and clearly defined diffusion profiles associated with adjacent grain boundaries, especially in the vicinity of biotite. As a consequence these are most amenable to estimating intergranular diffusion rates. Mg contents may plateau at different values along some garnet-quartz boundaries (Fig. 7). Low Mg contents of garnet adjacent to quartz are relatively unusual (Fig. 6c) and may be caused by interference with other diffusion profiles generated at grain boundaries in the matrix near to the studied interfaces. Background gradients in Mg content of garnet along and across muscovite-quartz grain boundaries may also reflect proximity to biotite (Fig. 8c). Mn and Fe variation is typically inversely correlated with the Mg contents, but Mn may be locally decoupled. Associated with the geochemical anomalies at the quartz-muscovite-garnet triple junctions, Mn may record relatively efficient intergranular diffusion in comparison to Mg. Thus in comparison to Mg, Mn profiles have shallower gradients especially between quartz and garnet (Fig. 8). The surface chemistry implies that Mn is transported preferentially to the garnet, perhaps sourced from nearby biotite, along grain boundaries between quartz and muscovite. This is apparently at odds with suggestions of relatively sluggish intergranular diffusion of Mn (Carlson *et al*., 2015a).

Ca shows complex long-wavelength, low-amplitude variations on the garnet surfaces and lacks the well-defined diffusion profiles that characterize Mg, Fe and Mn distribution. Adjacent to matrix plagioclase boundaries, garnet lacks evidence of diffusive exchange of Ca, and the geochemical profiles along these

boundaries are similar to the garnet-quartz boundaries. Most Ca variation is unrelated to the nature of the immediately adjacent mineral phase. Some garnet surfaces preserve low amplitude Ca-anomalies (both negative (Fig. 9) and positive (Fig. 7, 8)) that may be broadly correlated with the positions of the triple junctions of mineral boundaries. Although the long wavelength variations point to effective Ca transport relative to other cations, there is a lack of equilibrium, and variation is typically not related to either the positions of grain boundaries or the nature of the matrix phase. This could in theory represent:

a) a *partial late equilibration with a Ca-bearing fluid phase* (Carlson *et al.,* 2015a) with relatively effective transport processes. Hence as with the behaviour of Mg and Mn, this may be indicative preferential transport Ca along some of the triple junction grain boundaries. Potentially this could be linked to the presence an interconnected fluid network (Watson & Brenan, 1987) locally delivering cations to and from the garnet surface at the triple junctions. The triple junction-related effects are not present on all such boundaries implying either a crystallographic or structural control on the effectiveness of transport in these zones. Individual planar interfaces show just as much variation in Ca content as the apparent triple junction effects, which implies that transport processes at these interfaces was independent of the nature of the grain interface. This model fails to explain how both peaks and troughs in Ca content of the garnet surface could be generated on apparently identical planar grain boundaries and is not compatible with the presence of fluid on such boundaries. It is also thought unlikely that fluids would be present during the retrograde cooling.

b) a *compositional variation established during the initial growth of the garnet*. A general prograde surface heterogeneity may in part be a reflection of the relatively distal nature of Ca sources in the pelites and consequently low diffusive flux. This contrasts with the behaviour of Mg, Fe and Mn, which all exchange directly across interfaces with the relatively abundant ferro-magnesium minerals in the matrix. These elements are also readily available due to efficient volume diffusion within nearby biotite, which doesn't act as a rate limiting step for transport. Ca is only present in a few other phases in pelites, such as plagioclase, which doesn't appear to be involved in exchange reactions, and apatite which is only present as an accessory phase. Hence larger transport distances are required for Ca equilibration and the Ca contents of garnet surfaces are perhaps most likely to be difficult to equilibrate in pelites. Consequently the Ca variation is believed to represent a prograde growth feature established at higher temperatures than the retrograde diffusion profiles that characterise the other divalent cations. This would explain low amplitude, long wavelength variations that are decoupled from the present geometry of adjacent matrix phases.

Garnet porphyroblasts may preserve evidence for sluggish Ca intergranular diffusion (Chernoff & Carlson, 1997) but other studies demonstrate preferential equilibrium at low temperatures relative to the other major cations. The latter has been linked to increased solubility of Ca in the presence of a fluid phase (Carlson *et al*., 2015a). In the absence of such fluids, Ca equilibration may not occur until upper amphibolite facies conditions (Carlson, 2002). Intergranular diffusivity may drop by orders of magnitude if a network of fluids is absent

(Brenan, 1993). Fluids are likely to be largely absent during the establishment of the retrograde diffusion profiles. However it seems that Ca distribution will be more sensitive to other factors such as the presence of fluids and proximity to sources of Ca in pelites. In general the relative rates of intergranular diffusion along garnet-matrix interfaces suggest that Mn movement is more rapid than Mg and Fe, and intergranular equilibration of Ca is most difficult in this rock.

Estimation of intergranular diffusion rates

To enable the calculation of absolute values for diffusion rate it is crucial to have well constrained thermal histories of the samples. Such histories are not well established for the prograde, post-garnet growth histories of these Dalradian rocks, although evidence would suggest cooling histories were rapid (Dempster, 1985; Oliver *et al*., 2000). A range of different diffusivity data exists for volume diffusion in garnet with general agreement that Fe, Mg, and Mn diffusion coefficients and activation energies are broadly similar and Ca diffusion is significantly slower (Ganguly *et al*., 1998; Chakraborty & Ganguly, 1992; Carlson, 2006; Vielzeuf *et al*., 2007). However there remains uncertainty in the influence of garnet composition (Ganguly, 2010). The uncertainty associated with volume diffusion rates (Carlson, 2006; Ganguly, 2010) coupled to uncertainty in the detailed thermal histories of these rocks precludes reliable absolute estimates of intergranular diffusion rates in our study. However diffusion profiles may be used to give an indication of relative diffusion rates through a comparison of different element diffusion profiles and comparison with volume diffusion profiles. The compositional changes on these surfaces are more gradual along garnet-biotite boundaries than garnet-quartz boundaries. Hence intergranular diffusion is faster along garnet-biotite boundaries.

The Mg-volume diffusion profiles can be compared to the Mg-profiles for intergranular diffusion preserved on the garnet surfaces. Such an approach may not be justified for all cations given that volume diffusion requires simple multicomponent exchange (Borinski *et al*., 2012), whereas the grain boundary composition profiles potentially reflect more diffusive fluxes controlled by the proximity to sources of cations from other phases (Mueller *et al*., 2010). In addition the grain boundary profiles themselves will represent an integrated composition of garnet from a few microns below the surface rather than the diffusion pathway itself. It is also important to note that Mg-diffusion in garnet does not act independently and must be coupled to diffusion of at least one other divalent cation. Typically in the measured profiles, Mg exchange is maintained by both Mn and Fe variation. However the comparison undertaken here involves volume diffusion profiles in garnet adjacent to biotite with profiles along the garnet grain boundaries (with either quartz or plagioclase) away from adjoining biotite. As such the biotite provides a proximal source/sink for Mg-Fe. This approach (Fig. 9) demonstrates that Mg-diffusion profiles along the garnet-quartz grain boundaries and garnet-plagioclase grain boundaries are very similar to those of volume diffusion profiles within the garnet. These observations from polyphase boundaries contrast with experimental studies of Yb-Y coupled diffusion in garnet pairs (Marquardt *et al*., 2011) in which grain boundary transport is reported to be nearly 5 orders of magnitude faster than volume diffusion. In terms of the total amount of chemically modified garnet (i.e. the steepness of the diffusion profiles), Mg-diffusion along the plagioclase-garnet interface appears to be slowest, followed by the volume diffusion of Mg within garnet, whilst the rates of Mg-diffusion along the quartz-garnet interface are the

most effective of those presented in figure 9. Fitting diffusion curves to the profiles along the garnet-biotite boundaries are harder because of the relative lack of clearly defined diffusion profiles along the measured boundaries. However given the available data on the relatively short "clean" traverses that we have measured, we estimate that diffusion distances are at least 4 times greater than those of volume diffusion within garnet.

IMPLICATIONS

Grain boundaries are the key zones through which elemental transport occurs and metamorphic equilibration is facilitated. Hence intergranular diffusion has been suggested as "the most common impediment to equilibration" during metamorphism (Carlson, 2002) and as such is a key control on metamorphic processes. Snapping rocks along the mineral grain boundaries reveals important textural (Dempster *et al*., 2006; Lawther & Dempster, 2009) and chemical information regarding these zones. This study focuses on the chemical variations along garnet grain boundaries and represents the first time that intergranular diffusion profiles have been observed on natural mineral surfaces. It crucially emphasizes the importance of a different analytical approach to petrological research, one that is not based on thin section analysis.

Our study reveals that intergranular diffusion on garnet grain boundaries is typically slow, occurring at similar rates to volume diffusion in garnet. Previous studies of intergranular diffusion have suggested similarly sluggish transport along grain boundaries (Florence & Spear, 1995; O'Brien, 1999) on the basis of disequilibrium recorded in thin sections, although the role of fluid on the grain boundary interfaces in these scenarios has been questioned (Dohmen &

523 Chakraborty, 2003). However, many investigations suggest that intergranular
524 diffusion rates are faster by one or more orders of magnitude than rates of
525 volume diffusion (e.g. Farver & Yund, 2000; Milke *et al*., 2001). There is
526 significant variation in diffusion rates of different cations for different grain
527 boundary types. These types range from asymmetrical isolated boundaries
528 (Mishin & Razumovskii, 1992) to fast grain boundaries (Eiler *et al*., 1992) that
529 respectively apply to the garnet-biotite-quartz boundaries and the movement
530 along the triple junction network in our study.
531 Diffusion of divalent cations along boundaries involving quartz and plagioclase is
532 slow in comparison to movement along garnet-biotite boundaries. The lack of
533 Ca-exchange between plagioclase and garnet is notable. If as seems likely such
534 behaviour also characterizes low temperature prograde metamorphism it would
535 potentially compromise the application of geobarometers based on such
536 equilibria (Holdaway 2001; Wu *et al*., 2004). As such plagioclase appears to
537 behave as a closed system in these conditions, much in the way that muscovite
538 does in low-grade metamorphic environments (Dempster, 1992).
539 Crystallographic orientation also appears to play a role in the rate of
540 intergranular transport with faster Fe-Mg diffusion parallel to the [001] cleavage
541 in both muscovite and biotite. This is similar to, although less marked than, that
542 reported for anisotropic volume diffusion in biotite (Usuki, 2002). Although
543 preferential transport along some triple junctions of grain boundaries is
544 recorded, ineffective transport along the planar boundaries limits the impact of
545 these fast pathways in maintaining equilibrium on the garnet surface. Because of
546 the sluggish nature of intergranular diffusion, garnet surfaces are heterogeneous
547 and their chemistry is as much controlled by the availability, and proximity to

548 sources of cations, as it is to the rates of diffusion (Mueller *et al*., 2010). The
549 abundance of Fe- and Mg- bearing phases and their availability in the matrix of
550 pelites means that equilibrium is more readily achieved for these cations during
551 garnet growth. However for typical pelites it is predicted that Ca is most likely to
552 preserve heterogeneities on the garnet surface due to the lack of available Ca
553 sources in the matrix.
554 Given the sluggish nature of volume diffusion in garnet, similarly slow grain
555 boundary diffusion is likely to be a significant kinetic influence during prograde
556 metamorphism, especially that associated with relatively low temperature
557 conditions. The low temperatures of retrograde exchange favour grain boundary
558 chemical heterogeneity, and the inferred lack of fluids, due to the lack of
559 significant retrogression, may also reduce length scales of equilibration.
560 Prograde metamorphism is characterized by additional factors that will promote
561 equilibrium, particularly fluid release by dehydration reactions (Bell & Cuff,
562 1989) and penetrative deformation (Dempster & Tanner, 1997). The latter will
563 potentially allow fluid access and whilst fluid presence may enhance diffusion in
564 intergranular zones, some studies suggest this may not be the case (Farver &
565 Yund, 1995). High permeability of metamorphic basement rocks may be short-
566 lived, even during prograde events (Yardley & Valley, 1997; Yardley, 2009),
567 relative to the time-scales over which diffusion is effective. Consequently the
568 sluggish intergranular diffusion recorded during retrograde processes may also
569 be applicable to prograde metamorphism.
570 Low rates of grain boundary diffusion will inhibit garnet growth, and equilibrium
571 at the growing edge of the porphyroblast. The initial stages of garnet growth at
572 lower temperatures should be more sensitive to the nature of adjoining phases

than during growth at higher temperature. As such overprint zoning (Yang & Rivers, 2001; Hirsch *et al*., 2003) should be more commonly observed in examples of low temperature porphyroblast growth. Reports of overprint zoning in garnet porphyroblasts from the well-documented Harpswell Neck locality (Hirsch *et al*., 2003) point to sluggish intergranular diffusion of Mn and Mg during the early stages of prograde growth. Published X-ray maps of garnets from this locality show that locally high Mn and low Mg contents are associated with areas of relatively few quartz inclusions within the poikiloblasts (Hirsch *et al*., 2003; Carlson *et al*., 2015a). If this observation is correct it suggests that sluggish diffusion in the quartz-rich parts of the matrix inhibited chemical equilibration at the garnet margin. Other studies also appear to show a correlation between a lack of equilibrium in the zoning profiles and inclusion-rich areas of garnet porphyroblasts (O'Brien, 1999). Perchuk *et al*. (2009) suggest that Mg-Fe volume diffusion may be slowed by the presence of inclusions in comparison to inclusion-free garnet and our results suggest that the grain boundaries of these inclusions will not provide an effective transport system within porphyroblasts.

Intergranular diffusion is strongly controlled by the nature of the grain boundary and so garnet growth in layers with different modal proportions will occur at different rates. Initial growth of garnet may occur in finer grained chlorite-rich lithologies, and as such much of what garnet requires may be locally accessible. However disequilibrium garnet growth is reported in quartz-rich layers in comparison to more equilibrium growth and larger porphyroblasts in mica-rich domains (Spear & Daniel, 1998; Carlson *et al*., 2015a). This would be consistent

with the more effective intergranular diffusion on phyllosilicates grain boundaries in comparison to quartz grain boundaries.

The sharpest compositional changes on the garnet surfaces are associated with garnet-Fe-oxide, garnet-quartz and garnet-plagioclase grain boundaries. Hence intergranular diffusion will be sluggish during garnet growth adjacent to these phases. These minerals typically form the most common type of inclusion in garnet porphyroblasts and this may be a reflection of the difficulty in moving components along these grain margins (Yang & Rivers, 2001). Hence locally sluggish diffusion on the boundaries of garnet may have a fundamental control on the textures of porphyroblast growth.

SUMMARY

New techniques of porphyroblast surface analysis provide a means to quantify rates of intergranular diffusion on variety of different grain boundaries for a range of elements. Such rates when combined with established techniques that monitor scales of disequilibrium in garnet zoning and the distribution of porphyroblasts provide a powerful combination of tools with which to assess of the controls on metamorphic equilibration and porphyroblast growth. Models of metamorphic behaviour based on relatively slow intergranular diffusion rates would predict chemical disequilibrium of the garnet surface during porphyroblast growth with overprint zoning of cations dominant at low temperatures and in relatively quartz-rich lithologies. Divergence from such behaviour would be expected if intergranular diffusion is not the dominant kinetic impediment to the establishment of metamorphic equilibrium. Hence a lack of correlation between porphyroblast size and lithology may point to the

importance of other kinetic factors. Equally an apparent lack of matrix-related "overprint" growth zoning in garnet argues that either volume diffusion has smoothed out such growth features or that deformation (Bell & Hayward, 1991; Dempster & Tanner, 1997) and fluids (Rubie, 1986; Jamtveit *et al*., 1990; Pattison *et al*., 2011; Carlson *et al*., 2015a) may be of primary importance in enhancing elemental mobility during prograde metamorphism.

ACKNOWLEDGMENTS

We thank Dave Waters and Thomas Mueller for their careful and insightful reviews that significantly enhanced the manuscript.

REFERENCES

Ague, J.J. & Baxter, E.F., 2007. Brief thermal pulses during mountain building recorded by Sr diffusion in apatite and multicomponent diffusion in garnet. *Earth and Planetary Science Letters*, **261**, 500-516.

Barrow, G., 1893. On an intrusion of muscovite-biotite gneiss in the southeastern Highlands of Scotland and its accompanying metamorphism. *Quarterly Journal of the Geological Society, London*, **49**, 330-358.

Bell, T.H. & Cuff, C., 1989. Dissolution, solution transfer, diffusion versus fluid flow and volume loss during deformation/metamorphism. *Journal of Metamorphic Geology*, **7**, 425-447.

Bell, T.H. & Hayward, N., 1991. Episodic metamorphic reactions during orogenesis – the control of deformation partitioning on reaction sites and reaction duration. *Journal of Metamorphic Geology*, **9**, 619-640.

646 Borinski, S.A., Hoppe, U., Chakraborty, S., Ganguly, J. & Bhowmik, S.K., 2012.
647 Multicomponent diffusion in garnets I: general theoretical considerations and
648 experimental data for Fe-Mg systems. *Contributions to Mineralogy and Petrology*,
649 **164**, 571-586.
650 Brady, J.B., 1983. Intergranular diffusion in metamorphic rocks. *American Journal*
651 *of Science*, **283**, 181-200
652 Brenan, J.M., 1993. Diffusion of chlorine in fluid bearing quartzite: effects of fluid
653 composition and total porosity. *Contributions to Mineralogy and Petrology*, **115**,
654 215-224.
655 Bromiley, G.D. & Hiscock, M., 2016. Grain boundary diffusion of titanium in
656 polycrystalline quartz and its implications for titanium in quartz (TitaniQ)
657 geothermobarometry. *Geochimica et Cosmochimica Acta*, **178**, 281-290.
658 Caddick, M.J., Konopásek, J. & Thompson, A.B., 2010. Preservation of garnet
659 growth zoning and the duration of prograde metamorphism. *Journal of Petrology*,
660 **51**, 2327-2347.
661 Carlson, W.D., 1989. The significance of intergranular diffusion to the
662 mechanisms and kinetics of porphyroblasts crystallization. *Contributions to*
663 *Mineralogy and Petrology*. **103**, 1-24.
664 Carlson, W.D., 2002. Scales of disequilibrium and rates of equilibration during
665 metamorphism. *American Mineralogist*, **87**, 185-204
666 Carlson, W.D., 2006. Rates of Fe, Mg, Mn, and Ca diffusion in garnet. *American*
667 *Mineralogist*, **91**, 1-11
668 Carlson, W.D., Hixon, J.D., Garber, J.M. & Bodnar, R.J., 2015a. Controls on
669 metamorphic equilibration: the importance of intergranular solubilities
670 mediated by fluid composition. *Journal of Metamorphic Geology,* **33**, 123-146.

Carlson, W.D., Pattison, D.R.M. & Caddick, M.J., 2015b. Beyond the equilibrium paradigm: How consideration of kinetics enhances metamorphic interpretation. *American Mineralogist*, **100**, 1659-1667.

Carmichael, D.M., 1969. On the mechanism of prograde metamorphic reactions in quartz-bearing politic rocks. *Contributions to Mineralogy and Petrology*, **20**, 244-267.

Chakraborty, S. & Ganguly, J., 1992. Cation diffusion in aluminosilicate garnets: experimental determination in spessartine-almandine diffusion couples, evaluation of effective binary diffusion coefficients, and applications. *Contributions to Mineralogy and Petrology*, **111**, 74-86.

Chernoff, C.B. & Carlson, W.D., 1997. Disequilibrium for Ca during growth of pelitic garnet. *Journal of Metamorphic Geology*, **15**: 421-438.

Dempster, T.J., 1985. Garnet zoning and metamorphism of the Barrovian type area, Scotland. *Contributions to Mineralogy and Petrology*, **89**, 30-38.

Dempster, T.J., 1992. Zoning and recrystallization of phengitic micas: implications for metamorphic equilibration. *Contributions to Mineralogy and Petrology*, **109**, 526-537.

Dempster, T.J., Campanile, D. & Holness, M.B., 2006. Imprinted textures on apatite: a guide to paleoporosity and metamorphic recrystallization. *Geology*, **34**, 897-900.

Dempster, T. & Jess, S.A., 2015. Ikaite pseudomorphs in Neoproterozoic Dalradian slates record Earth's coldest metamorphism. *Journal of the Geological Society, London*, **172**, 459-464.

Dempster, T.J., Rogers, G., Tanner, P.W.G., Bluck, B.J., Muir, R.J., Redwood, S.D., Ireland, T.R. & Paterson, B.A., 2002. Timing of deposition, orogenesis and

696 glaciation within the Dalradian rocks of Scotland: constraints from U-Pb ages.
697 *Journal of the Geological Society, London*, **159**, 83-94.
698 Dempster, T.J. & Tanner, P.W.G., 1997. The biotite isograd, Central Pyrenees: a
699 deformation-controlled reaction. *Journal of Metamorphic Geology*, **15**, 531-548.
700 Dohmen, R. & Chakraborty, S. 2003. Mechanism and kinetics of element and
701 isotopic exchange mediated by a fluid phase. *American Mineralogist*, **88**, 1251-
702 1270.
703 Dohmen, R. & Milke, R., 2010. Diffusion in polycrystalline materials: grain
704 boundaries, mathematical models, and experimental data. *Reviews in Mineralogy*
705 *and Geochemistry*. **72**, 921-970.
706 Ehlers, K., Powell, R. & Stuewe, K., 1994. Cooling rate histories from
707 garnet+biotite equilibrium. *American Mineralogist*, **79**, 737-744.
708 Eiler, J.M., Baumgartner , L.P. & Valley, J.W., 1992. Intercrystalline stable isotope
709 diffusion – a fast grain-boundary model. *Contributions to Mineralogy and*
710 *Petrology*, **112**, 543-557.
711 Farver, J.R. & Yund, R.A., 1995. Grain boundary diffusion of oxygen, potassium
712 and calcium in natural and hot-pressed feldspar aggregates. *Contributions to*
713 *Mineralogy and Petrology,* **118**, 340-355.
714 Farver, J.R. & Yund, R.A., 2000. Silicon diffusion in a natural quartz aggregate:
715 constraints on solution-transfer diffusion creep. *Tectonophysics*, **325**, 193-205.
716 Florence, F.P. & Spear, F.S., 1991. Effects of diffusional modification of garnet
717 growth zoning on P-T path calculations. *Contributions to Mineralogy and*
718 *Petrology*, **107**, 487-500.

719 Florence, F. P. & Spear, F.S., 1993. Influences of reaction history and chemical
720 diffusion on P-T calculations for staurolite schists from the Littleton Formation,
721 northwestern New Hampshire. *American Mineralogist*, **78**, 345-359.
722 Florence, F.P. & Spear, F.S., 1995. Intergranular diffusion kinetics of Fe and Mg
723 during retrograde metamorphism of a pelitic gneiss from the Adirondack
724 Mountains. *Earth and Planetary Science Letters*, **134**, 329-340.
725 Ganguly, J., 2010. Cation diffusion kinetics in aluminosilicate garnets and
726 geological applications. *Reviews in Mineralogy and Geochemistry*, **72**, 559-601.
727 Ganguly, J., Cheng, W. & Chakraborty, S. 1998. Cation diffusion in aluminosilicate
728 garnets: experimental determination in pyrope-almandine diffusion couples.
729 Contributions to Mineralogy and Petrology, **131**, 171-180.
730 Harte, B. & Hudson, N.F.C., 1979. Pelite facies series and the temperatures and
731 pressures of Dalradian metamorphism in E Scotland. In: Harris, A.L., Holland, C.H.
732 & Leake, B.E., (eds) *The Caledonides of the British Isles reviewed*. Geological
733 Society of London Special Publications, **8**, 323-337.
734 Hirsch, D.M., Prior, D.J. & Carlson, W.D. 2003. An overgrowth model to explain
735 multiple, dispersed high-Mn regions in the cores of garnet porphyroblasts.
736 *American Mineralogist*, **88**, 131-141.
737 Holdaway, M.J. 2001. Recalibration of the GASP geobarometer in the light of
738 recent garnet and plagioclase activity models and versions of the garnet-biotite
739 geothermometer. *American Mineralogist*, **86**, 1117-1129.
740 Jamtveit, B., Bucher-Nurminen, K. & Austrheim, H. 1990. Fluid controlled
741 eclogitization of granulites in deep crustal shear zones, Bergen Arcs, Western
742 Norway. *Contributions to Mineralogy and Petrology*, **104**, 184-193.

743 Joesten, R.L., 1991. Grain boundary diffusion kinetics in silicate and oxide
744 minerals. In: *Diffusion, atomic ordering, and mass transport*. Ganguly, J., (ed)
745 Springer New York 345-395.
746 Kohn, M.J., 2003. Geochemical zoning in metamorphic minerals. In: *Treatise on*
747 *Geochemistry*, **3**, 229-261.
748 Kohn, M.J. & Spear, F., 2000. Retrograde net transfer reaction insurance for
749 pressure-temperature estimates. *Geology*, **28**, 1127-1130.
750 Kretz, R. 1983. Symbols for rock forming minerals. *American Mineralogist*, **68**,
751 277-279.
752 Lasaga, A.C., 1983. Geospeedometry: an extension of geothermometry. In:
753 Saxena, S.K., (ed) *Kinetics and equilibrium in mineral reactions*. Springer New
754 York, 81-114.
755 Lawther, S.E.M. & Dempster, T.J., 2009. Apatite grain boundary morphology and
756 its response to low-temperature fluid infiltration in crystalline basement.
757 *Geofluids*, **9**, 224-236.
758 Marquardt, K., Petrishcheva, E., Gardés, E., Wirth, R., Abart, R. & Heinrich, W.,
759 2011. Grain boundary and volume diffusion experiments in yttrium aluminium
760 garnet bicrystals at 1,723 K: a miniaturized study. *Contributions to Mineralogy*
761 *and Petrology*, **162**, 739-749.
762 Milke, R., Wiedenbeck, M. & Heinrich, W., 2001. Grain boundary diffusionof Si, Mg
763 and O in enstatite reaction rims: a SIMS study using isotopically doped reactants.
764 *Contributions to Mineralogy and Petrology*, **142**, 15-26.
765 Mishin, Y.M. & Razumovskii, I.M., 1992. Analysis of an asymmetrical model for
766 boundary diffusion. *Acta Metallurgica et Materialia*, **40**, 597-606.

767 Mueller, T., Watson, E.B. & Harrison, T.M., 2010. Applications of diffusion data to
768 high-temperature Earth systems. *Reviews in Mineralogy and Geochemistry.* **72**,
769 997-1038.
770 Müller, T., Massonne, H-J. & Willner, A.P., 2015. Timescales of exhumation and
771 cooling inferred by kinetic modeling: An example using a lamellar garnet
772 pyroxenite from the Variscan Granulitgebirge, Germany. *American Mineralogist*,
773 **100**, 747-759.
774 O'Brien, P.J., 1999. Asymmetric zoning profiles in garnet from HP-HT granulite
775 and implications for volume and grain-boundary diffusion. *Mineralogical*
776 *Magazine*, **63**, 227-238.
777 Okudaira, T., Bando, H. & Yoshida, K., 2013. Grain-boundary diffusion rates
778 inferred from grain-size variations of quartz in metacherts from a contact
779 aureole. *American Mineralogist*, **98**, 680-688.
780 Oliver, G.J.H., Chen, F., Buchwaldt, R. & Hegner, E., 2000. Fast
781 tectonometamorphism and exhumation in the type area of Barrovian and Buchan
782 zones. *Geology*, **28**, 459-462.
783 Pattison, D.R.M., De Capitani, C. & Gaidies, F., 2011. Petrological consequences of
784 variations in metamorphic reaction affinity. *Journal of Metamorphic Geology,* **29**,
785 953-977.
786 Pattison, D.R.M. & Tinkham, D.K., 2009. Interplay between equilibrium and
787 kinetics in prograde metamorphism of pelites: an example from Nelson aureole,
788 British Columbia. *Journal of Metamorphic Geology,* **27**, 249-279.
789 Perchuk, A.L., Burchard, M., Schertl, H-P., Maresch, W.V., Gerya, T.V., Bernhardt,
790 H-J. & Vidal, O. 2009. Diffusion of divalent cations in garnet. *Contributions to*
791 *Mineralogy and Petrology*, **157**, 573-592.

792 Reed, S.J.B., 2005. *Electron microprobe analysis and scanning electron microscopy*
793 *in geology.* Cambridge University Press. 189pp.
794 Rubie, D.C., 1986. The catalysis of mineral reactions by water and restrictions on
795 the presence of aqueous fluids during metamorphism. *Mineralogical Magazine*,
796 **50**, 399-415.
797 Sorby, H.C., 1851. On the microscopical structure of the Calcareous Grit of the
798 Yorkshire coast. *Quarterly Journal of the Geological Society of London,* **7**, 1-6.
799 Spear, F.S., 1988. Metamorphic fractional crystallization and internal
800 metasomatism by diffusional homogenization of zoned garnets. *Contributions to*
801 *Mineralogy and Petrology*, **99**, 507-517
802 Spear, F.S., 1991. On the interpretation of peak metamorphic temperatures in the
803 light of garnet diffusion during cooling. *Journal of Metamorphic Geology*, **32**, 903-
804 914.
805 Spear, F.S. & Daniel, C.G., 1998. Three-dimensional imaging of garnet
806 porphyroblasts sizes and chemical zoning: nucleation and growth history in the
807 garnet zone. *Geological Materials Research*, **1**, 1-44.
808 Tracy, R.J., 1982. Compositional zoning and inclusions in metamorphic minerals.
809 *Reviews in Mineralogy and Geochemistry*, **10**, 355-397.
810 Usuki, T., 2002. Anisotropic Fe-Mg diffusion in biotite. *American Mineralogist*, **87**,
811 1014-1017.
812 Vernon, R.H., 2004. *A practical guide to rock microstructure.* Cambridge
813 University Press, 594pp.
814 Vielzeuf, D., Baronnet, A., Perchuk, A.L., Laporte, D. & Baker, M.B., 2007. Calcium
815 diffusivity in alumino-silicate garnets: an experimental and ATEM study.
816 *Contributions to Mineralogy and Petrology*, **154**, 153-170.

817 Viete, D.R., Hermann, J., Lister, G.S. & Stenhouse, I.R., 2011. The nature and origin
818 of the Barrovian metamorphism, Scotland: diffusion length scales in garnet and
819 inferred thermal time scales. *Journal of the Geological Society, London,* **168**, 115-
820 132.
821 Vorhies, S.H. & Ague, J.J., 2011. Pressure-temperature evolution and thermal
822 regimes in the Barrovian zones, Scotland. *Journal of the Geological Society,*
823 *London*. **168**, 1147-1166.
824 Watson, E.B. & Brenan, J.M., 1987. Fluids in the lithosphere, 1. Experimentally-
825 determined wetting characteristics of CO_2-H_2O fluids and their implications for
826 fluid transport, host-rock physical properties, and fluid inclusion formation.
827 *Earth and Planetary Science Letters*, **85**, 497-515.
828 Whitney, D.L., Goergen, E.T., Ketcham, R.A. & Kuze, K., 2008. Formation of garnet
829 polycrystals during metamorphic recrystallization. *Journal of Metamorphic*
830 *Geology,* **26**, 365-383.
831 Woodsworth, G.J., 1977. Homogenization of zoned garnets from pelitic schists.
832 *Canadian Mineralogist*, **15**, 230-242.
833 Wu, C-M., Zhang, J. & Ren, L-D., 2004. Empirical garnet-biotite-plagioclase-quartz
834 (GBPQ) geobarometry in medium- to high-grade metapelites. *Journal of*
835 *Petrology*, **45**, 1907-1921.
836 Yang, P. & Rivers, T., 2001. Chromium and manganese zoning in pelitic garnet
837 and kyanite: spiral, overprint, and oscillatory (?) zoning patterns and the role of
838 growth rate. *Journal of Metamorphic Geology,* **19**, 455-474.
839 Yardley, B.W.D., 1977. An empirical study of diffusion in garnet. *American*
840 *Mineralogist*, **62**, 793-800.

Yardley, B.W.D., 2009. The role of water in the evolution of the continental crust. *Journal of the Geological Society, London*, **166**, 585-600.

Yardley, B.W.D. & Valley, J.W., 1997. The petrologic case for a dry lower crust. *Journal of Geophysical Research*, **102**, 12173-12185.

FIGURE LEGENDS

Figure 1. Transmitted light photomicrograph showing rounded morphology of garnet porphyroblast containing Fe-oxide and quartz inclusions aligned at an angle to the external muscovite-rich fabric. Note the presence of brown Fe-staining on some fractures and grain boundaries.

Figure 2. X-ray maps for (a) Mg, (b) Mn, and (c) Ca variation within a garnet porphyroblast. (d) Mg concentration traverses (X_{prp}) through the edge of a garnet porphyroblast adjacent to biotite. Traverse is oriented perpendicular to the garnet edge.

Figure 3. Low magnification electron microscope images of the surface of a garnet porphyroblast and its adjacent matrix. (a) Secondary electron image of garnet, dashed area shows the high magnification area shown in (b) and (c); (b) High magnification secondary electron image of part of the garnet surface shown in (a); (c) Backscattered electron image of the garnet surface shown in image (b); (d) Backscattered electron image of the matrix surface adjacent to the garnet surface shown in (b), this image is reversed so that grain boundary positions in the matrix may be matched to positions on the garnet surface. Labels (Kretz, 1983) identify the matrix minerals.

866

867 *Figure 4*. Secondary electron image of garnet porphyroblast surface showing flat
868 grain boundary areas, prominent ridges associated with growth steps and
869 variable development of irregular Fe-oxide coating, shown by brighter patches
870 (marked by arrows). Wherever possible chemical traverses of the garnet
871 surfaces avoided these topographic features and later deposits.

872

873 *Figure 5*. X-ray maps of (a) Fe and (b) Al composition of garnet porphyroblast
874 surface. Positions of matrix phase boundaries adjacent to the garnet surface are
875 shown in figure (a) with outlined in white dashed line the position of an Fe-oxide
876 grain within the adjacent matrix. Note that the high Fe content of the garnet
877 surface adjacent to biotite in the lower left hand area of the X-ray map is due to a
878 locally thick Fe-surface coating.

879

880 *Figure 6.* Major element cation traverses (in % of end member composition) of
881 garnet surfaces across the position of quartz-biotite grain boundaries (shown by
882 dashed red lines). Pairs of backscattered images of the garnet and the reversed
883 image of the adjacent matrix show the positions of each traverse. Each pair of
884 images is positioned above the corresponding compositional traverse. Position of
885 the matrix grain boundary is marked on the line of traverse by the red dashed
886 line. (a) Traverse (A-B) perpendicular to orientation of biotite cleavage; (b)
887 Traverse (C-D) perpendicular to biotite cleavage trace. “Noise” in sections of this
888 traverse adjacent to biotite reflect the presence of particularly coarse Fe-oxide
889 surface deposits on the garnet-biotite boundary; (c) Traverse (E-F) parallel to

890 the orientation of the biotite cleavage trace. Note this traverse was analysed over
891 a shorter time period and as a consequence errors are a little larger.
892
893 *Figure 7.* Major element cation traverses (in % of end member composition) of
894 garnet surface across an adjacent biotite-plagioclase grain boundary. Location of
895 traverse (G-H) shown in backscattered electron images of the garnet and the
896 reversed image of the adjacent matrix.
897
898 *Figure 8.* Major element cation traverses (in % of end member composition) of
899 garnet surface across adjacent quartz-muscovite grain boundaries. Location of
900 traverses shown in backscattered electron images of the garnet and the reversed
901 image of the adjacent matrix. (a) Traverse (I-J) parallel to the orientation of the
902 muscovite cleavage; (b) Traverse (K-L) perpendicular to the muscovite cleavage.
903
904 *Figure 9*. Comparison of Mg diffusion profiles for garnet grain boundaries with
905 volume diffusion profile (from Figure 2d) within porphyroblast (red dashed
906 line). Garnet surface diffusion profiles for garnet-quartz boundary (green dotted
907 line; A-B in figure 6) and garnet-plagioclase boundary (blue, dashed-dotted line;
908 G-H in figure 7). Inset shows schematic positions of diffusion profiles (coloured
909 arrows) in thin section view of grain boundaries with all traverses shown
910 oriented away from a garnet-biotite boundary. Volume diffusion profile shown is
911 truncated 2 μm from the grain edge due to potential uncertainty in the true
912 composition caused by the volume of interaction with the electron beam.

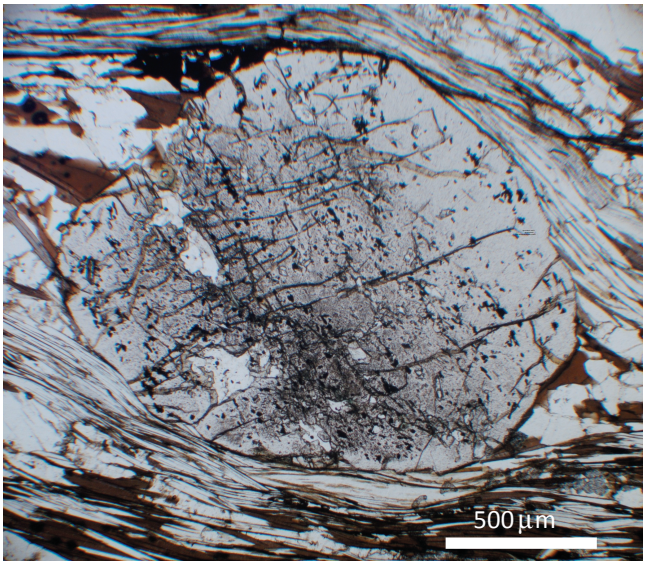

Dempster et al (Fig 1)

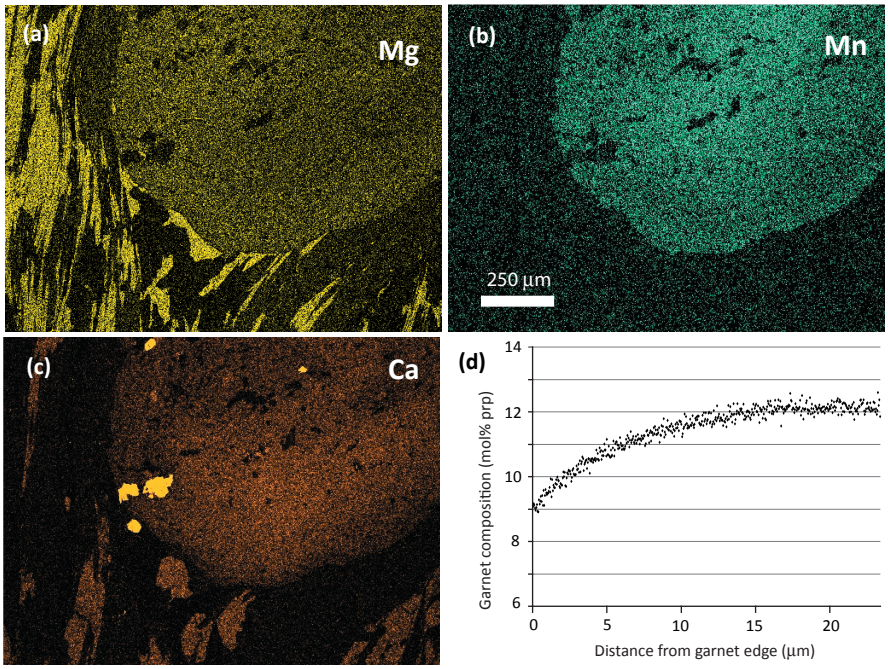

Dempster et al (Fig 2)

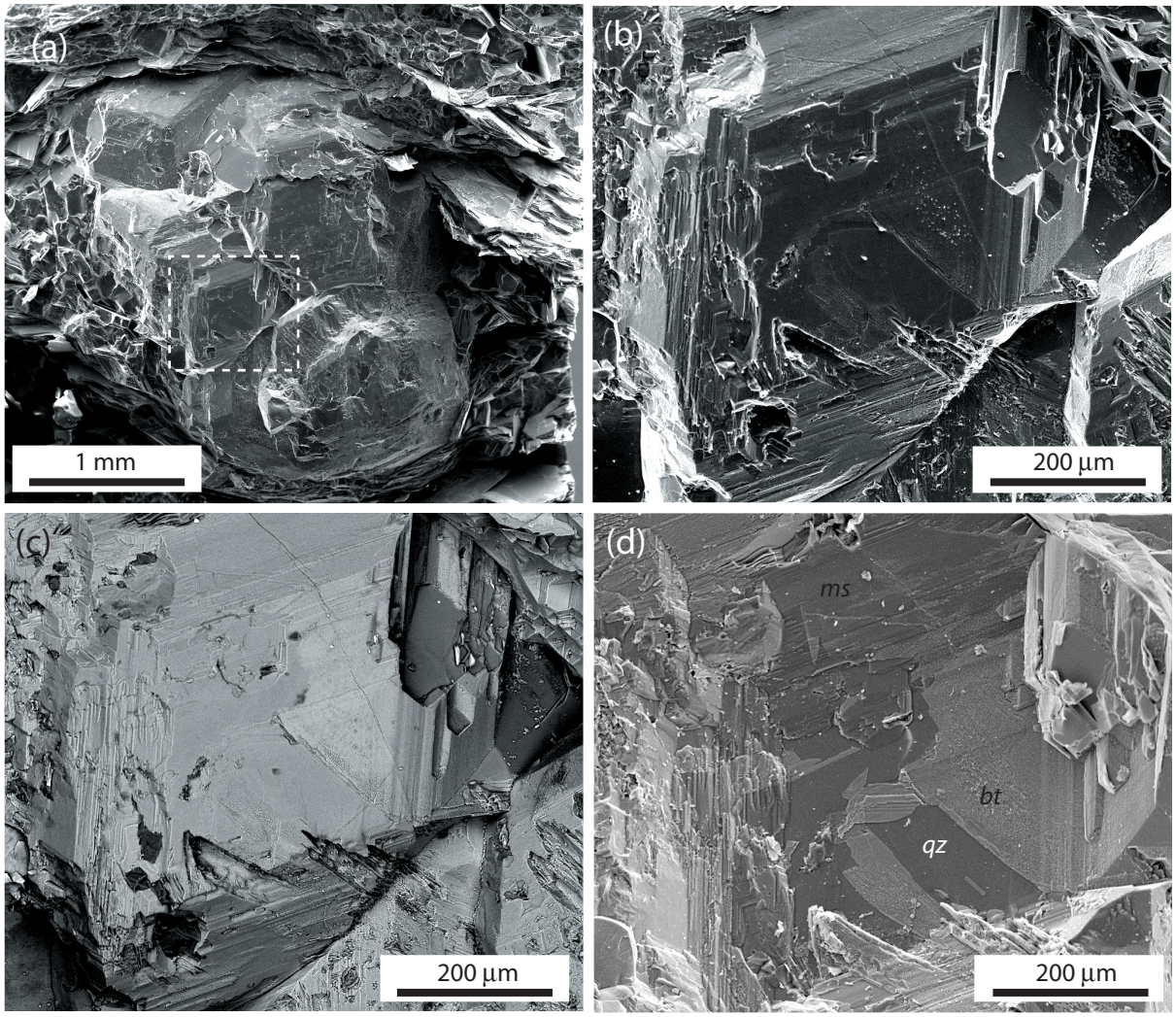

Dempster et al (Fig 3)

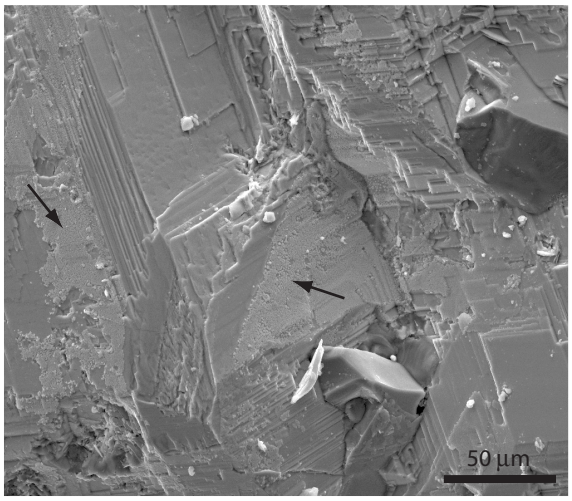

Dempster et al (Fig 4)

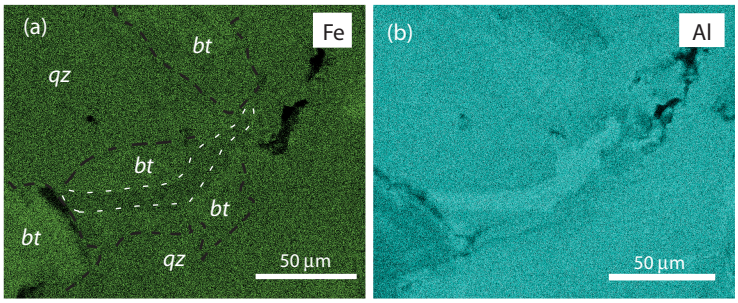

Dempster et al (Fig 5)

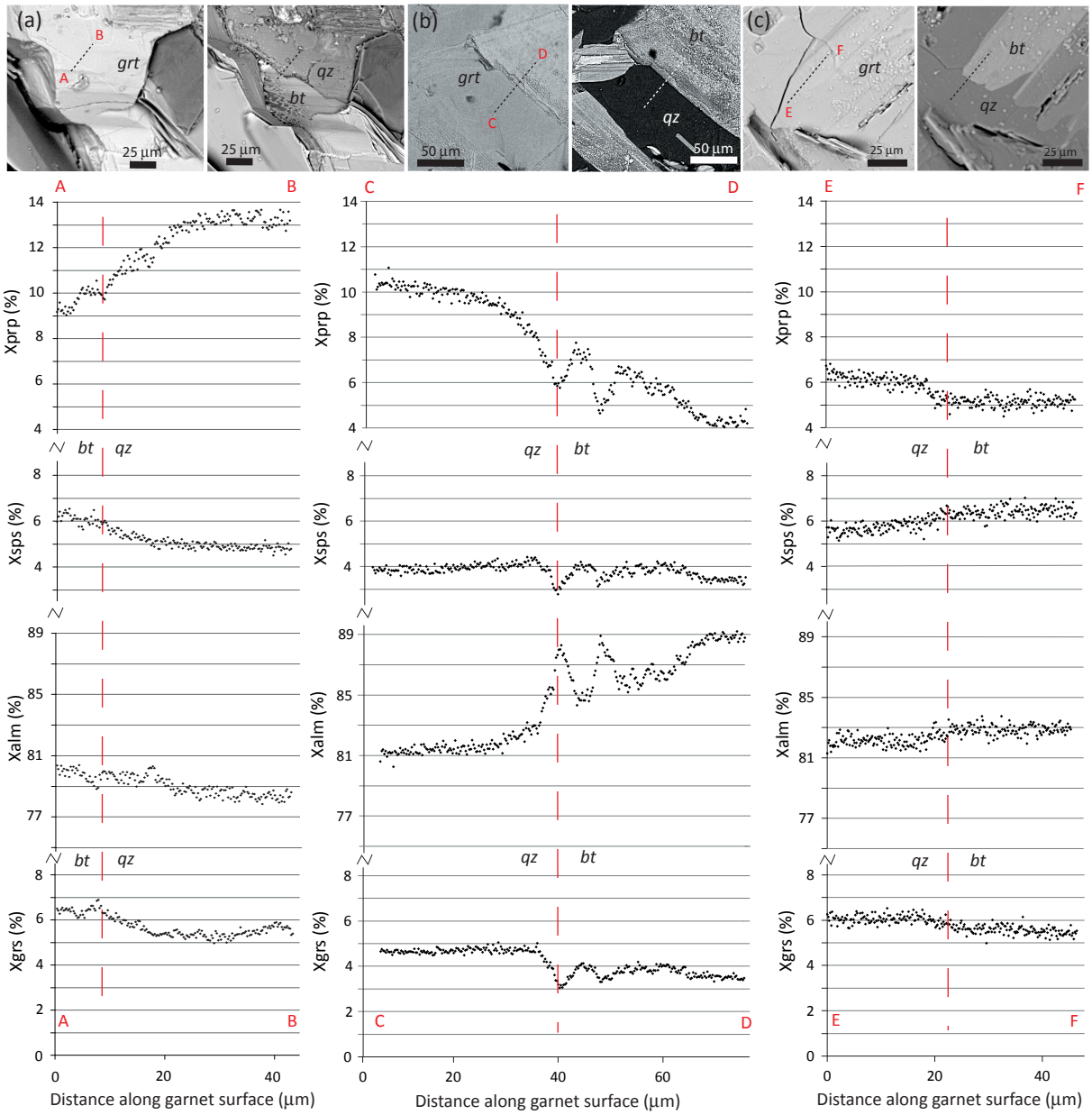

Dempster et al (Fig 6)

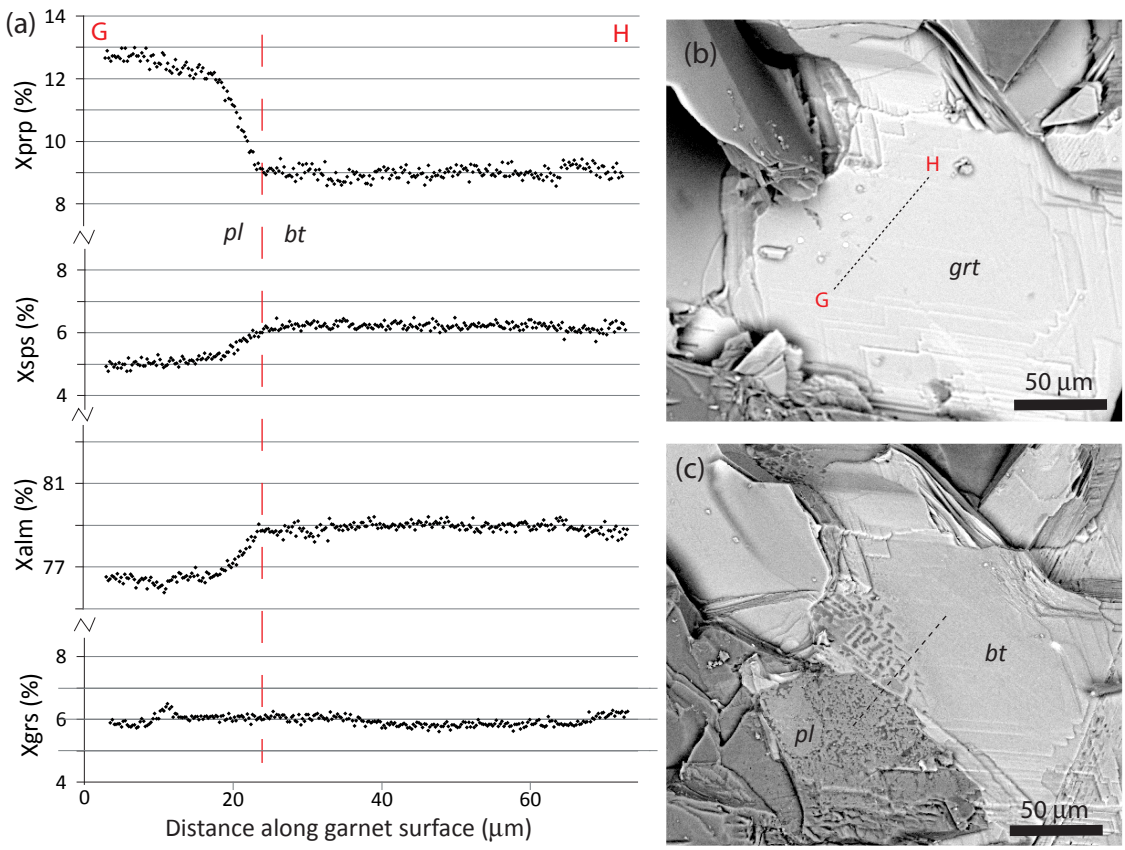

Dempster et al (Fig 7)

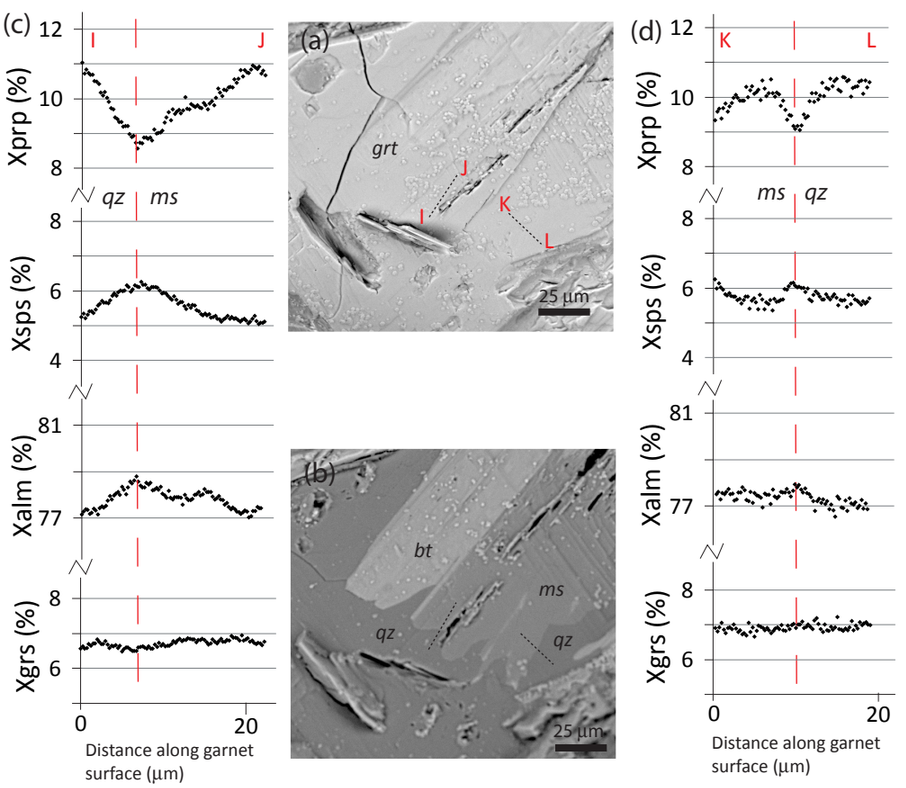

Dempster et al (Fig 8)

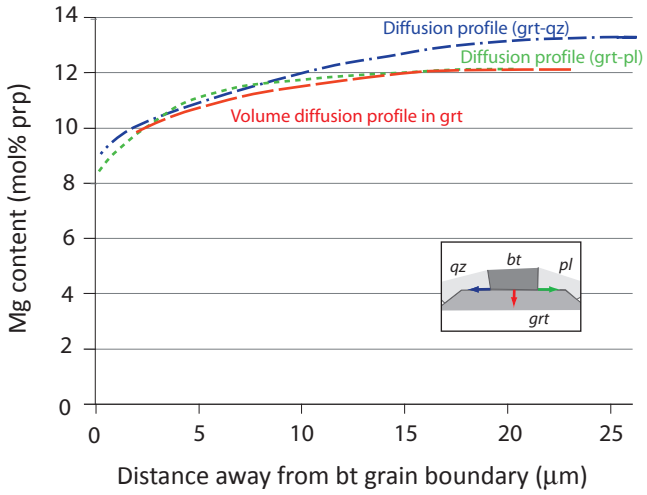

Dempster et al (Fig 9)